Model studies of the kinetics of collisional population transfer between dark and radiating excited electronic states: CaO(A′1Π)+N2OCaO(A 1Σ+)+N2O

Millard H. Alexander and Michael G. Osmolovsky

Citation: The Journal of Chemical Physics **77**, 839 (1982); doi: 10.1063/1.443900
View online: http://dx.doi.org/10.1063/1.443900
View Table of Contents: http://scitation.aip.org/content/aip/journal/jcp/77/2?ver=pdfcov
Published by the AIP Publishing

Model studies of the kinetics of collisional population transfer between dark and radiating excited electronic states: $CaO(A'\,^1\Pi)+N_2O \rightleftarrows CaO(A\,^1\Sigma^+)+N_2O$

Millard H. Alexander[a] and Michael G. Osmolovsky

Department of Chemistry, University of Maryland, College Park, Maryland 20742
(Received 16 March 1982; accepted 9 April 1982)

In a previous article [J. Chem. Phys. 76, 429 (1982)] we presented a model for collisional energy transfer between dark ($A'\,^1\Pi$, $a\,^3\Pi$) and radiating ($A\,^1\Sigma^+$) excited electronic states of the alkaline earth oxides. The inelastic transitions result from coupling between the electric dipole of the collision partner and a transition dipole in the alkaline earth oxide, which arises from the non-Born–Oppenheimer coupling between the rovibronic manifolds of two different electronic states. Here we use the rate constants reported in the previous article to investigate population flow from the nominally $v = 6$ manifold of the $A'\,^1\Pi$ state of CaO into the nominally $v = 0$ manifold of the $A\,^1\Sigma^+$ state, induced by collisions with N_2O. The master equation is solved in the steady state limit. The resulting populations are then used to simulate the pressure dependence of the (0–0) band of the CaO $A\,^1\Sigma^+ \rightarrow X\,^1\Sigma^+$ spectrum, and investigate the variation of the predicted spectral features with respect to changing the conditions which characterize both the rate of formation of the excited states as well as the rate of translational loss out of the zone of observation. At low to moderate target gas pressure the major effect of collisions is $A' \rightarrow A$ population transfer in the region of the largest coupling between the two rotational manifolds. The concomitant intensity increase and the spectral variation in the A state emission are qualitatively similar to features seen in experimental spectra of Irvin and Dagdigian, which we present here. The pressure dependent changes in the emission spectra are extremely sensitive to the assumed rate of translational loss, which must be taken into account in any comparison between experiments carried out under flame and molecular beam conditions. Finally, we demonstrate that although it is possible to fit with a simple two-level kinetic model the observed pressure dependence of the total A state emission, summed over rotational lines, the resulting kinetic parameters which characterize this fit may bear little relation to those which characterize the master equation for the coupling between the underlying rotational manifolds.

I. INTRODUCTION

In many reactions of alkaline earth atoms with molecular oxidants the exoergicities are large enough to allow formation of the alkaline earth oxide products in one or more of four low-lying excited states, namely $^{1,3}\Pi$ and $^{1,3}\Sigma^+$.[1–20] Of these, only the $A\,^1\Sigma^+$ state has a strong transition moment to the ground state.[21–23] Experimental studies of the pressure dependence of the total chemiluminescence yield[2,7,8,18–20] indicate that inelastic collisions, subsequent to the initial formation of products, transfer population from one or more of the dark excited states ($^{1,3}\Pi$, $^3\Sigma^+$) into the radiating $A\,^1\Sigma^+$ state.[9,11,18]

In a previous paper,[24] which we will refer to as I, we have presented a mechanistic model for this collisional energy transfer, based on the long-range coupling between the permanent dipole moment of a collision partner and the transition dipole between the electronic states of the alkaline earth oxide. This transition dipole arises primarily from the non-Born–Oppenheimer coupling of the rovibronic manifolds of two different electronic states. The coupling, which results from the presence of the orbit-rotation and spin-orbit terms in the full Hamiltonian, is significant only in the region of near degeneracy, where the rotational ladders of the two states become nearly isoenergetic. As we have shown by means of calculations for CaO, the rate constants for population transfer can be sizeable ($k > 1\times10^{-10}$ cm^3/molecule s) over a relatively narrow range of rotational quantum numbers around the $^1\Pi - {}^1\Sigma^+$ and $^3\Pi_0 - {}^1\Sigma^+$ isoenergetic points. We expect that at low to moderate pressure, population transfer will occur through these "rotational windows." At higher pressures this process will be augmented by rotational relaxation within the dark states, which will act to transfer population into the rotational windows.

With the rate constants determined in our earlier work it is possible to set up the master equation for the flow of population between the two coupled rotational manifolds. By solution of this equation one can simulate the pressure dependence of the chemiluminescence. In experiments in which production of the electronically excited species is continuous, a steady state solution of the master equation is appropriate. The kinetic model developed and applied here is similar in spirit to steady state models which have appeared in the literature.[18,25–28] An additional degree of sophistication is achieved here by the explicit inclusion of all the rotational levels of each of the vibrational states which are coupled both by non-Born–Oppenheimer perturbations and by collisions, while in these previous models the entire rotational manifold of each electronic state is treated as one level. The present model is applied to the particular case of population transfer from the $A'\,^1\Pi$ state to the $A\,^1\Sigma^+$ state of CaO. Our interest in this system is motivated by the recent molecular beam study by Irvin and Dagdigian[7,8] of the pressure dependence of the CaO $A\,^1\Sigma^+ - X\,^1\Sigma^+$ chemiluminescence subsequent to the reaction of $Ca(^3P, {}^1D)$ atoms with N_2O.

[a]Author to whom reprint requests should be addressed.

 0021-9606/82/140839-15$02.10

The organization of this paper is as follows: In the next section we discuss the mixing between the rotational manifolds of the $A\,^1\Sigma^+$ and $A'\,^1\Pi$ states due to the orbit-rotation perturbation. Section III summarizes the determination of the inelastic cross sections resulting from the dipole–dipole coupling between the CaO and N_2O molecules. The collision dynamics are treated within the microreversible Born approximation,[24,29] as described in Sec. I. The inelastic cross sections can be converted into thermal rate constants, which can be used in the appropriate master equation. This equation and its steady state solution are discussed in Sec. IV. Section V shows how the resulting collision induced population changes can be used to predict the expected changes in the molecular emission spectra. The actual implementation of the kinetic model is discussed in Sec. VI. We concentrate specifically on the study of the pressure dependence of the (0–0) band of the CaO $A\,^1\Sigma^+ \rightarrow X\,^1\Sigma^+$ spectrum. We investigate, to some degree, the variation in the predicted spectral features and intensities with respect both to changing the ratio of the initial formation rates of the A' and A states and to changing the rate of translational loss out of the zone of observation. The latter variation allows us to simulate both molecular beam and flame experiments. The calculated population changes and simulated spectra are presented in Secs. VIII and IX. The pressure variation of the integrated intensities is discussed in Sec. X, and a comparison is made with the predictions of a simple two-level steady state model. A concluding section compares the simulated spectra with experimental spectra obtained by Irvin and Dagdigian[8] and raises some implications of the present study for the interpretation of experiments.

II. MIXING OF BORN-OPPENHEIMER STATES

Consider $^1\Sigma^+$ and $^1\Pi$ states which are eigenfunctions of the Born–Oppenheimer Hamiltonian. The orbit-rotation term in the full molecular Hamiltonian will mix the $^1\Sigma^+$ state with the $^1\Pi$ state of e parity,[30] which is the following linear combination of the $\Lambda = \pm 1$ components[31]:

$$|JMv\,^1\Pi_e\rangle = 2^{-1/2}[|J, \Omega = 1, Mv, \Lambda = 1\rangle + |J, \Omega = -1, Mv, \Lambda = -1\rangle], \quad (1)$$

where J is the total angular momentum with projections along space- and molecule-fixed axis systems of M and Ω, respectively. Here v denotes the vibrational quantum number and Λ, the projection along the molecular axis of the electronic angular momentum. Since we will be dealing here exclusively with singlet states, spin labels have been suppressed.

The matrix element of the orbit-rotation term is diagonal in J and M and is given by[21]

$$\langle JMv_\Pi\,^1\Pi_e|H_{OR}|JMv_\Sigma\,^1\Sigma^+\rangle = -[2J(J+1)]^{1/2} b\,\langle v_\Pi|B|v_\Sigma\rangle\,. \quad (2)$$

Here $\langle v_\Pi|B|v_\Sigma\rangle$ denotes the off-diagonal (in both electronic and vibrational quantum numbers) matrix element of the rotational constant $B = \hbar^2/2\mu r^2$ and b is a strength constant, whose magnitude can be determined spectroscopically and which is defined as the matrix element of the electronic orbital angular momentum operator L_+, namely[32,33]

$$b = \langle {}^1\Pi, \Lambda = 1|L_+|{}^1\Sigma^+\rangle\,. \quad (3)$$

We have kept the notation of Field[21] but with the phase convention of Gottscho, Koffend, and Field.[32] The other Λ doubled $^1\Pi$ component $^1\Pi_f$ is not directly mixed with a $^1\Sigma^+$ state.[21,24]

For the alkaline earth oxides the orbit-rotation matrix elements are relatively small in magnitude. As a consequence the mixing between $^1\Pi_e$ and $^1\Sigma^+$ Born–Oppenheimer wave functions will be significant only if a near resonance occurs between the rotational ladders of the $^1\Pi$ and $^1\Sigma^+$ states. From the existence of spectral perturbations[21] we know that for each of the low-lying vibrational levels of the $A\,^1\Sigma^+$ state in CaO, SrO, and BaO, isoenergetic points occur with the rotational ladders of several vibrational levels of the $A'\,^1\Pi$ state. In the present paper we shall consider only the mixing between the $v_\Sigma = 0$ level of the $A\,^1\Sigma^+$ state of CaO and $v_\Pi = 6$ level of the $A'\,^1\Pi$ state. The isoenergetic point occurs at a rotational quantum number of $J \simeq 53$. The location of the other isoenergetic points, corresponding to different v_Σ, v_Π vibrational pairs, is illustrated in Fig. 1 of I.

We designate the eigenfunctions of the full Hamiltonian as $|JM+\rangle$ and $|JM-\rangle$, respectively, where[24]

$$|JM\pm\rangle = C_J^\pm|JMv_\Sigma\,^1\Sigma^+\rangle + D_J^\pm|JMv_\Pi\,^1\Pi_e\rangle\,. \quad (4)$$

As discussed in I, the coefficients are obtained by diagonalization of a 2×2 matrix and are related by

$$D_J^+ = (1 - C_J^{+2})^{1/2}\,, \quad (5a)$$

$$C_J^- = D_J^+\,, \quad (5b)$$

and

$$D_J^- = -C_J^+\,. \quad (5c)$$

The corresponding eigenvalues will be denoted as $E_J^\pm$. We will associate, arbitrarily, the minus sign with the higher energy. Except very near the isoenergetic point the predominant character of the full eigenfunctions will be either $^1\Sigma^+(|C_J| > |D_J|)$ or $^1\Pi(|C_J| < |D_J|)$. Since for CaO the $A\,^1\Sigma^+$ state has a larger rotational constant than the $A'\,^1\Pi$ state, a crossing of the two rotational ladders will occur only if the $^1\Sigma^+$ state is the lower energy member of each J pair below the isoenergetic point.

The reader should remember that the $|JM\pm\rangle$ states [Eq. (4)] are stationary eigenfunctions of the full Hamiltonian for the diatomic molecule, so that the $C_J^\pm$ and $D_J^\pm$ coefficients do not show any time dependence, other than an overall phase factor $\exp(-iE_J^\pm/\hbar)$ which is identical for both coefficients.

III. RATE CONSTANTS FOR COLLISIONAL POPULATION TRANSFER

In paper I we discussed in detail how collisions with a polar target gas can induce transitions between the various $|JM\pm\rangle$ states. Let us designate both the $|+\rangle$ or $|-\rangle$ indices by the index α. In a time-dependent formulation of the collision dynamics the amplitude for a

transition between states $|J_a M_a \alpha\rangle$ and $|J'_a M'_a \alpha'\rangle$, accompanied by a transition of the target from state $|J_b M_b\rangle$ to state $|J'_b M'_b\rangle$, is a function of the impact parameter. We shall assume that orientation effects are not important, in which case the essential inelastic quantity is the unpolarized transition probability, which is given by[29,34–37]

$$P_{J_a\alpha J_b \to J'_a\alpha' J'_b}(b) = [(2J_a+1)(2J_b+1)]^{-1} \times \sum_{\substack{M_a M'_a \\ M_b M'_b}} |A_{J_a M_a \alpha J_b M_b \to J'_a M'_a \alpha' J'_b M'_b}(b)|^2 . \quad (6)$$

The integral cross section is obtained by integration over the impact parameter

$$\sigma_{J_a\alpha J_b \to J'_a\alpha' J'_b} = 2\pi \int_0^\infty b\, P_{J_a\alpha J_b \to J'_a\alpha' J'_b}(b)\, db . \quad (7)$$

In paper I we discussed how numerical values of the transition probabilities can be obtained within the first Born approximation, and how this method can be modified[24,29] to ensure that the transition probabilities satisfy statistical microreversibility, which requires

$$(2J_a+1)(2J_b+1)P_{J_a\alpha J_b \to J'_a\alpha' J'_b} = (2J'_a+1)(2J'_b+1)P_{J'_a\alpha' J'_b \to J_a\alpha J_b} . \quad (8)$$

Thermal rate constants can be determined from the integral cross section of Eq. (7) by integration over an assumed Maxwellian distribution of relative velocities for the CaO+ target system, namely,[38]

$$k_{J_a\alpha J_b \to J'_a\alpha' J'_b}(T_t) = \left[\frac{8}{\pi m (kT_t)^3}\right]^{1/2} \int_0^\infty \sigma_{J_a\alpha J_b \to J'_a\alpha' J'_b}(E)\, E\, e^{-E/kT_t}\, dE , \quad (9)$$

where m is the collision reduced mass and T_t is the assumed translational temperature. The individual rate constants satisfy the usual detailed balance relation[39]

$$(2J'_a+1)(2J'_b+1)\exp[-(\epsilon'_a+\epsilon'_b)/kT_t]\, k_{J'_a\alpha' J'_b \to J_a\alpha J_b}(T_t) = (2J_a+1)(2J_b+1)\exp[-(\epsilon_a+\epsilon_b)/kT_t]\, k_{J_a\alpha J_b \to J'_a\alpha' J'_b}(T_t) . \quad (10)$$

where ϵ_a and ϵ_b denote the rotational energies of states $|J_a M_a \alpha\rangle$ and $|J_b M_b\rangle$, respectively.

In experiments in which only the states of the alkaline earth oxide are resolved, the appropriate rate constants can be obtained from Eq. (9) by summing and averaging over a distribution of target rotational states. If a Boltzmann distribution is assumed, with rotational temperature T_r, we have[29]

$$k_{J_a\alpha \to J'_a\alpha'}(T_t) = z_b^{-1}(T_r) \sum_{J_b, J'_b} (2J_b+1)\exp(-\epsilon_b/kT_r)\, k_{J_a\alpha J_b \to J'_a\alpha' J'_b}(T_t) , \quad (11)$$

where z_b denotes the rotational partition function of the target gas. With Eqs. (10) and (11) it is easy to show that the thermal rate constant for the reverse process $J'_a\alpha' \to J_a\alpha$ can be expressed as

$$k_{J'_a\alpha' \to J_a\alpha}(T_t) = \frac{(2J_a+1)}{(2J'_a+1)} \exp[(\epsilon'_a-\epsilon_a)/kT_t]\, z_b^{-1} \sum_{J_b J'_b} (2J_b+1) \times \exp[(\epsilon'_b/T_t - \epsilon'_b/T_r - \epsilon_b/T_t)/k]\, k_{J_a\alpha J_b \to J'_a\alpha' J'_b}(T_t) . \quad (12)$$

If the rotational and translational temperatures are equivalent $T_r = T_t$, then Eq. (12) reduces to a detailed balancing relation similar to Eq. (10) but bearing only the indices of molecule a, namely,

$$k_{J'_a\alpha' \to J_a\alpha}(T_t) = [(2J_a+1)/(2J'_a+1)]\exp[(\epsilon'_a-\epsilon_a)/kT_t]\, k_{J_a\alpha \to J'_a\alpha'}(T_t) . \quad (13)$$

Within a time-dependent treatment of the collision dynamics, as was carried out in I, the relative velocity is assumed to be constant, which is equivalent to assuming that the factor kT_t is large compared to the inelastic energy gaps. If this assumption is applied to Eq. (12), we can neglect the factors $(\epsilon'_a-\epsilon_a)/kT_t$ and $(\epsilon'_b-\epsilon'_b)kT_t$ to obtain

$$k_{J'_a\alpha' \to J_a\alpha}(T_t) = \frac{(2J_a+1)}{(2J'_a+1)} z_b^{-1}(T_r) \sum_{J_b J'_b} (2J_b+1) \times \exp(-\epsilon'_b/kT_r)\, k_{J_a\alpha J_b \to J'_a\alpha' J'_b}(T_t) , \quad (14)$$

which, however, is *not* identical to Eq. (13).

IV. COLLISION INDUCED POPULATION CHANGES

With the thermal rate constants defined by Eq. (11) we are now in a position to model collision induced changes in the populations of the mixed Born–Oppenheimer states defined in Sec. II above. Specifically, consider a situation in which the alkaline earth oxide is produced by a beam of metal atoms impinging on a static oxidant gas. Then the time evolution of the population density in level $|J\alpha\rangle$, where we recall that the index α will denote either of the $|+\rangle$ or $|-\rangle$ states, can be described by the master equation

$$\frac{dN_{J\alpha}}{dt} = \sigma_{J\alpha} F_b N_T - N_{J\alpha}\left(k_{J\alpha}^{\rm rad} + k_{\rm loss} + N_T \sum_{J'\alpha'} k_{J\alpha \to J'\alpha'}\right) + N_T \sum_{J'\alpha'} N_{J'\alpha'} k_{J'\alpha' \to J\alpha} . \quad (15)$$

Here F_b is the beam flux, $\sigma_{J\alpha}$ is the cross section for formation of state $J\alpha$, N_T is the target gas number density, $k_{J\alpha \to J'\alpha'}$ and $k_{J'\alpha' \to J\alpha}$ denote the collisional rate constants defined by Eq. (11), $k_{J\alpha}^{\rm rad}$ is the radiative rate of the $J\alpha$ level, and $k_{\rm loss}$ is the effective rate for translational loss of alkaline earth oxide out of the zone of observation. More will be said below about the latter two quantities.

In the present article we shall investigate the steady state solution of Eq. (15), which will be appropriate in the analysis of experiments where the excited states are produced in a continuous manner, as for example in many molecular beam or flame experiments.

To solve the resulting inhomogeneous linear equations we first rewrite the formation cross sections as

$$\sigma_{J\alpha} = p_{J\alpha}\sigma , \quad (16)$$

where σ is the total cross section for production of ex-

cited states, which is in principle experimentally accessible,[40] and $p_{J\alpha}$ is the fractional probability for production of the specific level $J\alpha$. If the target gas pressure is so low that collisional energy transfer does not occur, then the steady state populations are given by

$$N^0_{J\alpha} = N_T F_b \sigma p_{J\alpha} / (k^{\rm rad}_{J\alpha} + k^0_{\rm loss}) \ . \tag{17}$$

Here the superscript on the translational loss rate indicates the value appropriate to the low pressure limit, where product molecules do not suffer any collisions within the observation zone. Note that the factor $N_T F_b \sigma$ on the right-hand side of Eq. (17) is independent of the particular $J\alpha$ state and has the dimensions of a first-order rate constant (time^{-1}). The *relative* steady-state populations can be defined from Eq. (17) by dividing through by the common formation rate constant $N_T F_b \sigma$. These relative populations will be denoted by $n^0_{J\alpha}$. We will assume that the beam flux is independent of N_T, i.e., that there is no attenuation upstream.

In the presence of energy transfer collisions the relative steady state populations can be expressed in terms of the zero collision values as

$$n_{J\alpha} = f_{J\alpha} n^0_{J\alpha} \ , \tag{18}$$

where the quantities $f_{J\alpha}$ denote the populations relative to the zero collision limit, and where

$$N_{J\alpha} = N_T F_b \sigma n_{J\alpha} \ . \tag{19}$$

Substitution of Eqs. (18) and (19) into Eq. (15) and division by the common factor of $N_T F_b \sigma$ leads to a set of simultaneous equations for the fractional population changes. In matrix notation we have

$$\mathbf{R} f = -p \ , \tag{20}$$

where f and p are vectors with elements $f_{J\alpha}$ and $p_{J\alpha}$ respectively, and the elements of the matrix R are given by

$$R_{JJ} = -p_J \left(k^{\rm rad}_J + k_{\rm loss} + N_T \sum_{J'}{}' k_{J\to J'} \right) \Big/ (k^{\rm rad}_J + k^0_{\rm loss}) \tag{21}$$

and

$$R_{JJ'} = p_{J'} N_T k_{J'\to J} / (k^{\rm rad}_{J'} + k^0_{\rm loss}) \ , \tag{22}$$

where for simplicity the dual indices $J\alpha$ and $J'\alpha'$ have been simplified to J and J' in these two equations. In Eq. (21) the prime on the summation indicates that the term with $J' = J$ is omitted.

The present formulation implies that one can solve for the relative populations independent of a knowledge of the metal atom flux, which is often difficult to determine. Note that the value of the translational loss rate which appears in the numerator of Eq. (21) is not indexed by a superscript naught and is the rate appropriate to a particular experimental arrangement with target gas present at number density N_T.

V. CHANGES IN LUMINESCENCE SPECTRUM

In many experiments the production of electronically excited alkaline earth oxides is monitored by observation of the resulting luminescence. Each of the mixed Born–Oppenheimer states will give rise to a series of P and R branch lines corresponding to $A\,^1\Sigma^+(v_\Sigma) \to X\,^1\Sigma^+(v'')$ transitions at frequencies

$$\nu^P_{J\alpha} = [T_{v_\Sigma, v''} + E^\alpha_J - B_{v''}(J+1)(J+2)]/\hbar \tag{23}$$

and

$$\nu^R_{J\alpha} = [T_{v_\Sigma, v''} + E^\alpha_J - B_{v''} J(J-1)]/\hbar \ . \tag{24}$$

Here $B_{v''}$ is the rotational constant of the $X\,^1\Sigma^+$ state and $T_{v_\Sigma, v''}$ is the $A(v_\Sigma) \to X(v'')$ electronic term. We recall that the energies of the mixed states E^+_J are measured with respect to the v_Σ, $J = 0$ level of the A state, and that the index α in Eqs. (23) and (24) denotes either of the $|+\rangle$ or $|-\rangle$ mixed states. The relative intensities of these lines are given by[41]

$$I^P_{J\alpha}(\nu^P_{J\alpha}) = (J+1) n_{J\alpha} (h\nu^P_{J\alpha}) k^{\rm rad}_{J\alpha} / (2J+1) \tag{25}$$

and

$$I^R_{J\alpha}(\nu^R_{J\alpha}) = J n_{J\alpha} (h\nu^R_{J\alpha}) k^{\rm rad}_{J\alpha} / (2J+1) \ . \tag{26}$$

Since the populations which appear here are the relative steady-state populations [Eqs. (18) and (19)], the intensities are relative intensities, so that it is not necessary to multiply by the usual fundamental constants and by the $A \to X$ Franck–Condon factors.[33,41] The restriction to relative intensities is not a serious drawback, because absolute intensities are not easily accessible experimentally.

Since the radiative lifetime of the $A\,^1\Sigma^+$ state is much shorter than the value for the $A'\,^1\Pi$ state,[42] we can accurately approximate the radiative rates in Eqs. (25) and (26) by multiplying the unmixed $A\,^1\Sigma^+$ state mixing coefficient in Eq. (4). We find

$$k^{\rm rad}_{J\alpha} \simeq C^{+2}_J \tau^{-1}_\Sigma \ , \tag{27}$$

where τ_Σ is the $A\,^1\Sigma^+$ radiative lifetime, assumed to be measured in an experiment not overly sensitive to the small subset of rotational levels which are strongly mixed with the $A'\,^1\Pi$ state.

VI. IMPLEMENTATION OF THE CALCULATIONS

In the numerical applications, to be presented below, we considered perturbational mixing between the $A\,^1\Sigma^+$ ($v_\Sigma = 0$) and $A'\,^1\Pi(v_\Pi = 6)$ states of CaO. All rotational levels with $0 \le J \le 95$ were included for both states. For each value of J_a there are four upward transitions which give nonvanishing cross sections within the Born approximation, namely $|J_a \pm\rangle \to |J_a + 1, \pm\rangle$ and $|J_a \pm\rangle \to |J_a + 1, \mp\rangle$. Thermal rate constants for these processes with N_2O as the collision partner were taken directly from I. The summation in Eq. (11) extended over target rotational states up to $J_b(J'_b) = 62$, which ensures convergence for a Boltzmann N_2O rotational distribution at $T_r = 300\,^\circ$K. The dependence of these rate constants on the initial rotational quantum number of CaO is illustrated in Fig. 1. Although, as discussed in Sec. III above, the rate constants for the downward transitions ($J_a \to J_a - 1$) can not be strictly related to the values for the upward transitions by the simple detailed balance relation contained in Eq. (13), actual comparison with calculated downward rates indicated that the discrepancy was only on the order of several percent and often less. Thus, for the purposes of the present simulation

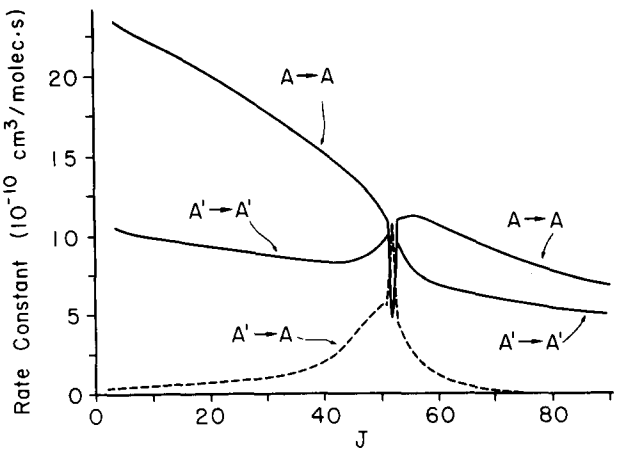

FIG. 1. Rate constants from Ref. 24 for upward ($J \rightarrow J'$) collisonal energy transfer among rotational levels of the (nominally) $A\,^1\Sigma^+(v=0)$ and $A'\,^1\Pi_e(v=6)$ manifolds of CaO in collisions with N_2O. The mixed Born–Oppenheimer states are denoted A and A' depending on their predominant character. For clarity the $A \rightarrow A'$ rates are not shown; they are similar to the $A' \rightarrow A$ values. Also for clarity the rates have been drawn as continuous curves although they are only defined for integer values of J. The isoenergetic point, where the mixing between the Born–Oppenheimer states is largest, occurs at $J=53$.

study we shall use Eq. (13) to calculate the downward rates, but with the translational temperature treated as a variable parameter, although logically the value should be fixed at 4800 °K, the temperature of the velocity distribution used in I to determine the upward rate constants from the cross sections.

Treating T_t as a variable parameter is not entirely unwarranted since our model does contain an inconsistency with respect to translational energy on the order of $\Delta E/kT_t$, where ΔE is a typical inelastic energy gap. This is because, as was discussed in Sec. III, in most impact parameter formulations of inelastic collision dyanmics[34–37] as, for example, the microreversible Born approximation used in I, conservation of energy is violated by the assumption of a constant velocity trajectory. Freeing T_t to be a variable parameter may also give our model additional flexibility to describe a physical situation which is in reality more complicated than the steady state picture we have presented. Our model includes only the relaxation of the nascent rotational distribution but does not treat the relaxation of the velocity distribution of the nascent products. This would require formulation and solution of the appropriate Boltzmann equation. Although this has been done for similar inelastic collision problems[43] the dimensionality of the present system would make such an approach difficult from a computational point of view. Consequently, the variation of T_t may be thought of as one approximate way of treating the relaxation of the translational energy. Obviously, then T_t should be given a value intermediate between the translational temperature of the nascent products (4800 K) and the translational temperature of the N_2O target gas (300 K in the experiments of Irvin and Dagdigian[7,8]). We expect that the effective relaxation of the translational energy will be more complete as the pressure of the target gas increases. As we shall see below, the predicted population changes are not sensitive to the particular choice of T_t within reasonable limits.

We turn now to a discussion of the effective rate for the translational loss of alkaline earth oxide molecules out of the zone of observation, which appears in Eq. (15). This rate could be thought of as the reciprocal of the residence time in the field of view. In molecular beam experiments such as those described by Dagdigian and co-workers,[5–8] in the zero collision limit the translational loss rate is just the reciprocal of the flight time. At finite target gas pressures this rate will decrease, although an exact prediction would involve solution of an extremely complicated, as well as poorly defined, transport problem.[44] As a compromise we assume that the loss rate obeys the simple form

$$k_{\rm loss} = k^0_{\rm loss}/(1+cP_T)\,, \tag{28}$$

where P_T is the target gas pressure and c is a constant. In a careful analysis of their particular experimental geometry Irvin and Dagdigian[7] deduced a value of $k^0_{\rm loss} = 2.55\times10^6$ s^{-1} and concluded that this rate would drop to 1.61×10^6 s^{-1} at an N_2O pressure of 0.3 Torr, which could correspond at a value for the constant c of 1.946 Torr.$^{-1}$. We shall use these values of c and $k^0_{\rm loss}$ here.

A radically different situation would characterize many flame experiments in which the observation zone is much smaller than the region in which products are formed, so that product molecules would be both entering and leaving the observation zone. In this case, a reasonable assumption is that the net translational loss rate will be equal to the flow velocity of the entrainment gas divided by the width of the image of the spectrometer slit projected back onto the flame. Assuming this dimension to be 0.1 cm and assuming a flow velocity of ~250 cm/s (~0.5% of the speed of sound), we predict a loss rate of $\sim 2.5\times10^3$ s^{-1}. Accordingly, in our simulation of population flow between the excited states of CaO under flame conditions, we adopted the same functional form [Eq. (28)] with the same value of the constant c but with $k^0_{\rm loss}$ reduced by a factor of 1000 to the value of 2.55×10^3 s^{-1}.

In order to model the population changes, as described in Sec. IV, it is first necessary to define the initial probabilities $p_{J\alpha}$ [Eq. (16)]. In one set of calculations we let this initial probability be a Kronecker delta. This would correspond to an experiment in which only one of the excited state levels was being produced, as would be the case if a cw dye laser was used to excite a beam of ground state alkaline earth oxide molecule. In another set of calculations we used a Boltzmann distribution to describe the initial population of the alkaline earth excited states. This would correspond to an experiment in which the excited alkaline earth molecules were being produced directly by chemical reaction, as in the experiments of Irvin and Dagdigian.[6–8] We shall assume that the relative population of each rotational level is given by the product of a Boltzmann distribution in the energy and a weight factor reflecting the relative size of the Born–Oppenheimer A

and A' components in the mixed state, i.e.,

$$p_{\alpha J} = (2J+1)\exp(-E_J^{\alpha}/kT_{\rm rot})[(C_J^{\alpha})^2 + w(D_J^{\alpha})^2] , \qquad (29)$$

where $T_{\rm rot}$ is an effective product rotational temperature. The parameter w represents the ratio of the overall production rate of the $A'\,^1\Pi(v_\Pi)$ manifold to that of the $A\,^1\Sigma^+(v_\Sigma)$ manifold. In the purely statistical limit[45] this factor will equal unity since, as was discussed in I, for CaO only the $A'\,^1\Pi$ rotational levels of e parity are strongly coupled by collisions to the $A\,^1\Sigma^+$ rotational manifold.[46] A Boltzmann distribution suffers from the disadvantage that energy conservation is violated at large J. Although this disadvantage can be corrected by the use of a rotational distribution based on information theory,[47] for example, this correction was not made in the present application, since the large exoergicity of the $Ca(^3P) + N_2O$ reaction, as studied in Dagdigian's laboratory,[5-7] implies that the energetic limit will occur for J values considerably larger than the upper limit of $J = 95$ used in the present study.[48]

VII. POPULATION CHANGES: BEAM CONDITIONS

Figures 2 and 3 display the steady state relative populations under conditions in which only the $J = 50$ and 52 levels of the nominally $A'\,^1\Pi$ state are initially populated. The isoenergetic point, where the maximum degree of mixing between the two Born–Oppenheimer states occurs, corresponds to $J = 53$. The populations are normalized to the steady-state population of the pumped level in the absence of any collisional energy transfer. The displayed populations correspond to three different pressures of the N_2O target. In all cases, the rate constant for translational loss was given by Eq. (28) with the values of the constants appropriate to molecular beam conditions.

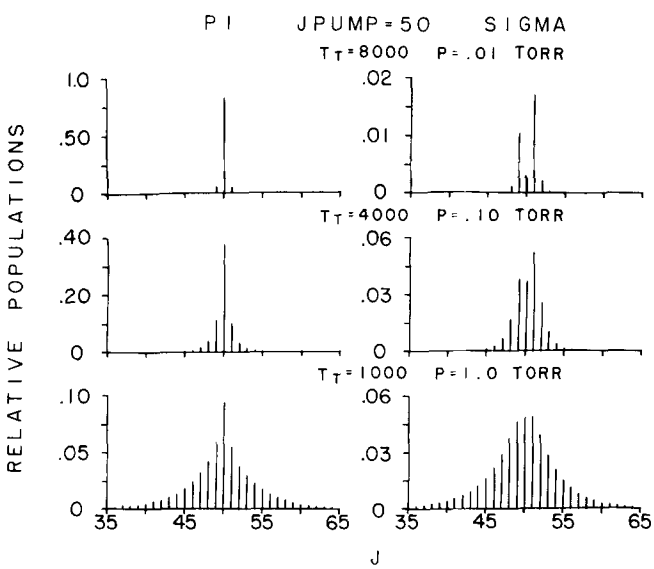

FIG. 2. Relative steady state populations of the mixed Born–Oppenheimer levels under conditions where the $J = 50$ level of the (norminally) $A'\,^1\Pi_e$ state is continuously pumped. The populations are normalized to the population of this level in the zero collision limit. The mixed levels are denoted "pi" and "sigma" depending on their dominant character. The zero pressure translation loss rate [Eq. (28)] was $2.55\times10^6\ s^{-1}$, the value appropriate to molecular beam conditions.

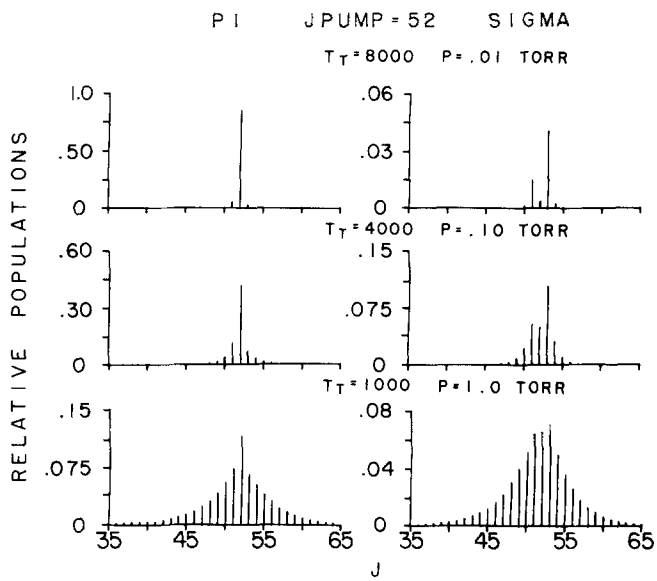

FIG. 3. Relative steady state populations of the mixed Born–Oppenheimer levels under conditions where the $J = 52$ level of the (nominally) $A'\,^1\Pi_e$ state is continuously pumped. The populations are normalized to the population of this level in the zero collision limit. The mixed levels are denoted "pi" and "sigma" depending on their dominant character. The zero pressure translational loss rate [Eq. (28)] was $2.55\times10^6\ s^{-1}$, the value appropriate to molecular beam conditions.

The behavior of the populations is not unexpected. At the higher pressures, the population of the pumped level, which is nominally $A'\,^1\Pi$ in character, tends to diffuse into neighboring $^1\Pi$ levels, an indication of rotational relaxation, or into neighboring $A\,^1\Sigma^+$ levels, an indication of interelectronic transfer. At very low pressure (0.01 Torr) the most populated $A\,^1\Sigma^+$ levels are those with $J = J_{\rm pump} \pm 1$. This is a direct reflection of the dipolar mechanism for the collisional population transfer (see I); the dipole selection rules imply that at least to first order the only nonvanishing cross sections correspond to the $J_a' = J_a \pm 1$ transition. As the pressure increases a greater number of collisional events begin to contribute to the steady-state populations, which tends to smooth out the dip in the (nominally) $A\,^1\Sigma^+$ state distribution at $J = J_{\rm pump}$. We see in Figs. 2 and 3 that the relative populations in the nominally $A\,^1\Sigma^+$ levels are roughly comparable to the populations in the $A'\,^1\Pi$ levels, except, of course, for the pumped level. This indicates that rotational relaxation (within the nominally $A'\,^1\Pi$ manifold) and interelectronic transfer ($A'\,^1\Pi \rightarrow A\,^1\Sigma^+$) are loss mechanisms of roughly equal importance.

The qualitative picture of the population changes becomes more complicated if the CaO excited states are assumed to be produced with the Boltzmann distribution described by Eq. (29). In this case it is convenient to examine the relative changes in the steady-state populations, which will be denoted as $\delta n_{J\alpha}$, where

$$\delta n_{J\alpha} = n_{J\alpha}/n_{J\alpha}^0 - 1 = f_{J\alpha} - 1 . \qquad (30)$$

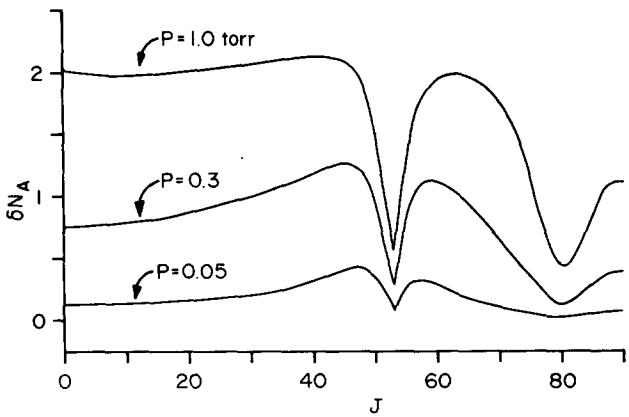

FIG. 4. Relative changes [Eq. (30)] in the population of the mixed Born–Oppenheimer states with an assumed A' to A production ratio of $w = 2$ [Eq. (29)]. Values are plotted only for those levels which are predominately $A\,^1\Sigma^+$ in character; this corresponds to the $|+\rangle$ (lower energy) levels for $J < 53$ and the $|-\rangle$ (higher energy) levels for $J \geq 53$. The rotational temperature of the nascent products [Eq. (29)] is 4000 K. The temperature parameter which appears in the detailed balancing relationship [Eq. (13)] is 4000 K for the curves at collisional pressures of 0.05 and 0.3 Torr and 1000 K for the $P = 1.0$ Torr curve. The zero collision translational loss rate [Eq. (28)] was taken to be 2.55×10^6 s^{-1}, the value appropriate to molecular beam conditions.

To get an idea of the magnitude of these changes we have have plotted in Fig. 4 the values of $\delta n_{J\alpha}$ as a function of J, obtained with a production ratio $w = 2$ [Eq. (29)], twice the ratio which would be predicted by a purely statistical treatment of the reactive collision dynamics. The graphed values are the relative changes for those levels which are nominally $A\,^1\Sigma^+$ in character.

This figure lends itself to a rather simple interpretation. Let us neglect rotational relaxation in the A and A' manifolds and consider a simplistic model wherein each A state level is coupled by collisions to a degenerate nonradiating level of the A' state. This two level model is equivalent in sophistication to many previous models used in the interpretation of experiments in which electronic energy transfer occurs.[18,25–28] The steady state solution of this type of two level model is presented in the Appendix. In the limit where the rate for collisional energy transfer is much larger than the translational loss rate, which will occur at high enough values of the pressure, the maximum relative change in the population of each A state level is given by Eq. (A7), which we reproduce here, namely,

$$\lim_{N_T k \gg k_{\rm loss}} \delta n_{J\alpha} = w + (1 + w) k^0_{\rm loss} / k_{\rm rad} \,. \tag{31}$$

This limit equals 3.275 for the values of w, $k_{\rm rad}$, and $k^0_{\rm loss}$ appropriate to Fig. 4. Examination of this figure indicates that for low J the values of $\delta n_{J\alpha}$ appear to be tending toward this limit. Very near the isoenergetic point ($J \sim 53$), the nominal A' levels acquire A state character through the orbit-rotation coupling. The A' levels can then radiate directly and do not serve as population reservoirs which can be tapped by a collisional mechanism. The minimum in the curves at $J \sim 80$ occurs because the net transition moment vanishes in this region,[24] so that even at substantial values of the collisional pressure there is no direct $A' \rightarrow A$ transfer. Finally, it is important to observe that at low pressure the largest population changes occur in the region of the isoenergetic point, where the rate constants for $A' \rightarrow A$ transfer are largest (Fig. 1).

VIII. LUMINESCENCE SPECTRA: BEAM CONDITIONS

The relative population changes were then used to simulate CaO $A\,^1\Sigma^+ \rightarrow {}^1\Sigma^+$ spectra, as described in Sec. V. We restricted ourselves to the 0–0 band, with origin at $\lambda = 865.9$ nm. A bandhead occurs in the R branch at $\lambda = 865.5$ nm ($J' = 11$) and the Franck–Condon factor is large (0.435).[49] Figure 5 presents two simulated stick spectra, the first for a hypothetically "pure" $A \rightarrow X$

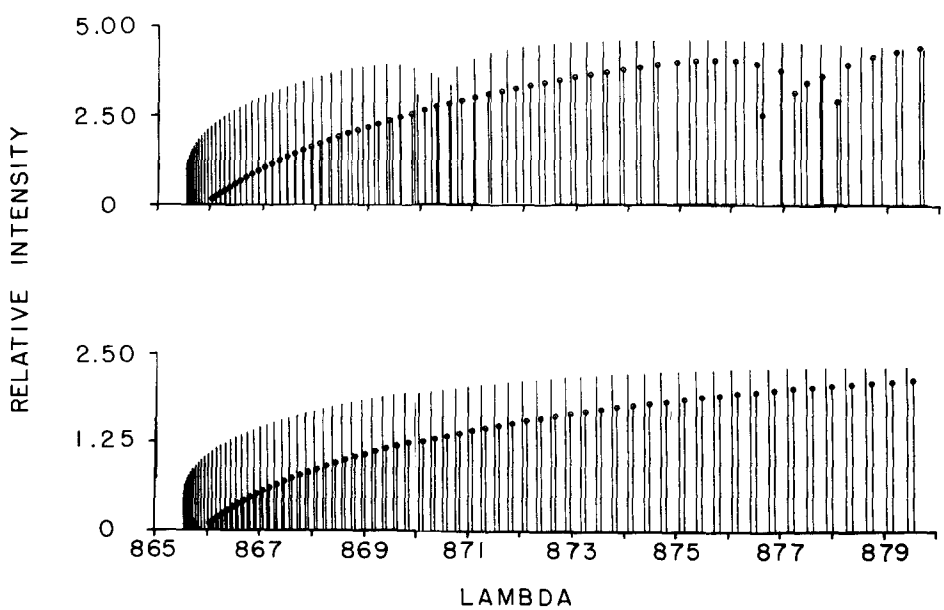

FIG. 5. Simulated steady-state $A\,^1\Sigma^+(v = 0) \rightarrow X\,^1\Sigma^+(v = 0)$ CaO spectra. The P branch lines are indicated by open circles. The rotational temperature of the nascent products [Eq. (29)] is 8000 K, the temperature parameter which appears in the detailed balancing relationship [Eq. (13)] is 1000 K, and the N_2O pressure is 1.0 Torr. The bottom trace corresponds to a hypothetically pure $A \rightarrow X$ band, obtained by neglecting both the orbit-rotation perturbation and the $A' \rightarrow A$ transfer. In both cases the spectra were arbitrarily normalized to the intensity of the zero-collision ($P = 0$) R branch line lying nearest to the wavelength $\lambda = 866$ nm. The zero-pressure translational loss rate was 2.55×10^6 s^{-1}, the value appropriate to molecular beam conditions.

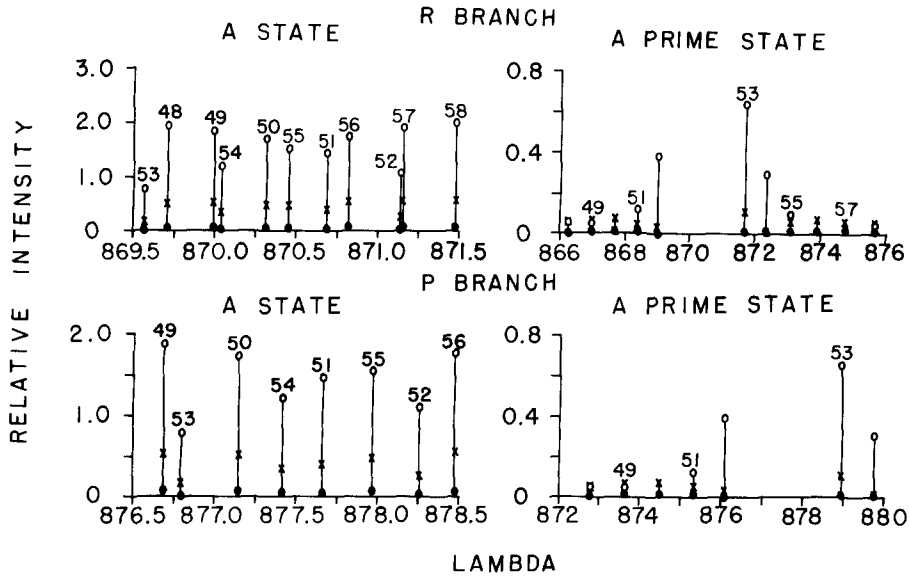

FIG. 6. Simulated steady-state $A\,^1\Sigma^+(V=0)\rightarrow X\,^1\Sigma^+(v=0)$ and $A'\,^1\Pi_e(v=6)\rightarrow X\,^1\Sigma^+(v=0)$ emission spectra in CaO. The rotational quantum number of the excited state is indicated. The two panels at the top and bottom display, respectively, the R branch lines and P branch lines originating from rotational levels near the isoenergetic point ($J=53$). For clarity, in both cases the overlapping lines of the other branch (Fig. 5) are not shown. The quantity plotted is the change in intensity relative to the zero-collision ($P=0$) intensity, normalized to the intensity of the zero-collision ($P=0$) R branch $A\,^1\Sigma^+$ state line lying nearest to the wavelength $\lambda=866$ nm. The intensity of the nominally $A'\,^1\Pi$ lines arises solely from intensity borrowing from the Born–Oppenheimer $A\,^1\Sigma^+$ state. The rotational temperature of the nascent products [Eq. (29)] was 8000 K and the zero-pressure translational loss rate was $2.55\times10^6\ s^{-1}$, the value appropriate to molecular beam conditions. The temperature parameter used in the detailed balancing relation [Eq. (13)] and the N_2O pressures were as follows: filled circles $T_t=8000$ K, $P=0.01$ Torr; crosses $T_t=4000$ K, $P=0.1$ Torr; open circles $T_t=1000$ K, $P=1.0$ Torr.

(0–0) band, obtained by setting the orbit-rotation perturbation equal to zero and neglecting all $A'\rightarrow A$ population transfer, and the second for the expected $A\rightarrow X$ (0–0) band, obtained by including both the orbit-rotation perturbation and the A'–A transfer rates. As is well known the perturbation leads to a displacement of the lines originating in excited state levels lying near the isoenergetic point ($J'=53$). The intensity changes will be discussed below.

Figure 6 presents in more detail the pressure dependence of the luminescence spectra of the levels in the region of the isoenergetic point, both for lines which originate in levels which are nominally $A\,^1\Sigma^+$ as well as nominally $A'\,^1\Pi_e$. Within our assumption that the radiative lifetime of the Born–Oppenheimer $A'\,^1\Pi$ state is much longer than that of the $A\,^1\Sigma^+$ state, the intensity of the nominally $A'\,^1\Pi$ lines in Fig. 6 is borrowed from the Born–Oppenheimer $^1\Sigma^+$ levels which are mixed in through the orbit-rotation perturbation.

The reader should note that the pressures mentioned here refer to the pressure (number density) of the collision partner which appears in Eqs. (21) and (22), so that variation of this "collisional" pressure can also be interpreted as a variation in the overall strength of the collisional coupling. In any experiment the formation rate in Eq. (15) $\sigma_{J\alpha}F_bN_T$ will also depend on the N_2O pressure. By neglecting this dependence, we can focus on collisional enhancement of chemiluminescence independent of the overall scaling resulting from an increase in the formation rate. Our simulated spectra could be compared with experimental spectra which have normalized with respect to N_2O pressure.

It is also worthwhile to examine the overall pressure dependence of the luminescence spectra under lower resolution. This can be achieved by convolution of the theoretically derived stick spectra (as in Fig. 5) with an assumed spectrometer slit width which we take to be triangular with a FWHM of 0.5 nm. The pure $A\rightarrow X$ 0–0 band, obtained as described in the first paragraph of this section, is displayed in Fig. 7 at a resolution of 0.2 nm. The rotational temperature of the nascent A

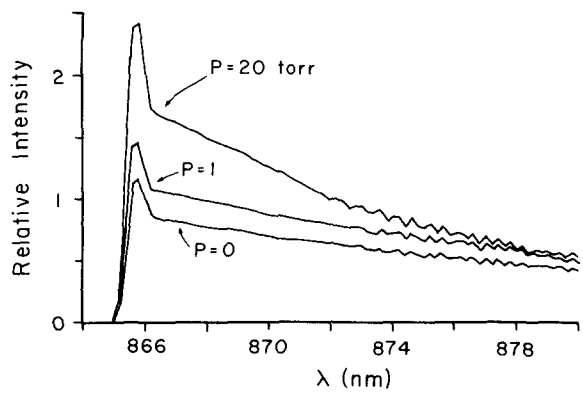

FIG. 7. Predicted low-resolution spectra for the pure $A\,^1\Sigma^+(v=0)\rightarrow X\,^1\Sigma^+(v=0)$ band at three collisional pressures, obtained by neglecting all $A'\rightarrow A$ collisional energy transfer. The spectra are all normalized to the $P=0$ intensity at $\lambda=866.0$ nm. The rotational temperature of the nascent products [Eq. (29)] was taken to be $2.55\times10^6\ s^{-1}$, the value appropriate to molecular beam conditions.

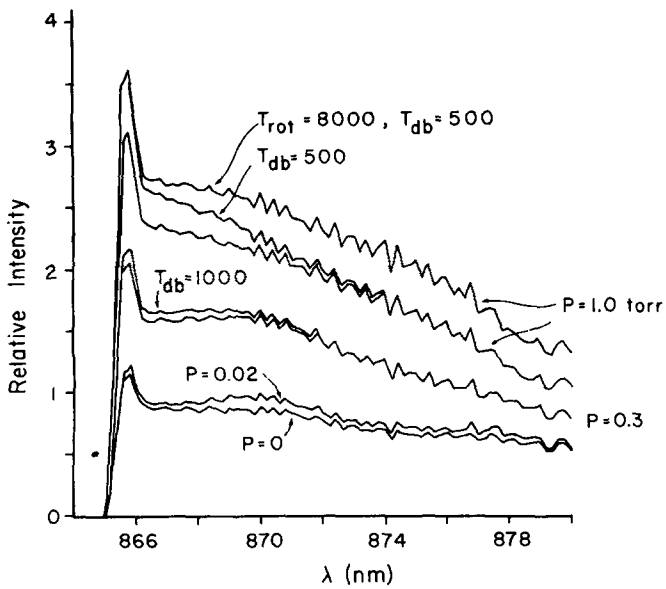

FIG. 8. $A\,^1\Sigma^+(v=0) \rightarrow X\,^1\Sigma^+(v=0)$ band spectra corresponding to an A' to A production ratio [Eq. (29)] of $w=2$. The product rotational temperature [Eq. (29)] and the detailed balancing temperature [Eq. (13)], denoted here by T_{db}, are both equal to 400 K unless another value is specified. All spectra are normalized to the $P=0$ intensity of $\lambda = 866$ nm. The zero collision translational loss rate [Eq. (28)] was taken to be $2.55\times10^6\ s^{-1}$, the value appropriate to molecular beam conditions.

state products [Eq. (29)] was taken to be 4000 K, which may underestimate slightly the population of the high rotational levels in experiments such as those of Irvin and Dagdigian[7,8] where the exoergicity for formation of the $v=0$ manifold of the A state is several eV. The translational temperature in the detailed balance relation [Eq. (13)] was 1000 K. The spectra are virtually insensitive to this quantity; more will be said about this later in this section. The spectra are all normalized to the zero collision ($P=0$) intensity at $\lambda = 866$ nm.

Examination of Fig. 7 shows a moderate increase in the relative height of the bandhead and of the region between 866 and 870 nm, which can be interpreted as evidence of rotational relaxation in the strongly polar A state. The increase in the overall intensity could be attributed also to rotational relaxation, which would transfer population from levels which radiate to the red of 880 nm (R lines with $J \rightarrow 82$, P lines with $J \rightarrow 60$) into levels which radiate in the spectral region examined. This is, however, unlikely to be the primary cause of the large increase in intensity seen in Fig. 7, since the radiative decay rate is so fast. If one assumes that the $A \rightarrow A$ relaxation rate is $\sim 1.5\times10^{-9}$ cm^3/molecule s (Fig. 1), then even at a pressure of 20 Torr only 7–8 J changing collisions will occur during the radiative lifetime of the A state. More likely the major factor behind the increase in integrated intensity is the decrease in the translational loss rate [Eq. (28)], which is 0.43 of the radiative decay rate at $P=0$, but drops to only 1% of k^{rad} at $P=20$ Torr.

We now contrast these spectra with those obtained when mixing with the $A'(v=6)$ level is allowed. Representative spectra are displayed in Fig. 8, obtained with a production ratio $w=2$ [Eq. (29)], which, as discussed before, is twice the ratio predicted by a purely statistical treatment of the reactive collision dynamics.[45] Because of this factor, even in the absence of collisions the perturbational mixing between the Born–Oppenheimer A' and A states will allow the latter to borrow population, and thus intensity, from the A' state with its larger nascent population.[50] This explains the enhancement of the $P=0$ spectrum in Fig. 8 over the $P=0$ spectrum in Fig. 7. The largest difference between the two $P=0$ spectra occurs in the region of $\lambda = 870$ nm. This is not surprising since the strongest perturbational mixing of the states occurs at the isoenergetic point ($J=53$) and since the $R(53)$ line lies at $\lambda = 870$ nm.

As seen in Figs. 2 and 3, at low pressures collision transfer will occur most readily in the region of the isoenergetic point where the $A' \rightarrow A$ rate constants are largest (Fig. 1). This explains why in Fig. 8 the largest difference between the $P=0$ and $P=0.02$ Torr spectra lies in the region of $\lambda = 870$ nm. At higher pressures not only does the intensity rise dramatically but also the hump centered at $\lambda = 870$ nm disappears. This suggests that $A' \rightarrow A$ transfer is occurring more uniformly over the entire rotational manifold, which agrees with our analysis of Figs. 2–4. The overall intensity rises much faster with increasing collisional pressure than in the case of the pure A state spectra in Fig. 7. This clearly demonstrates that collisions can effectively transfer population from the dark A' state into the radiating A state.

For collisional pressures of 0.3 and 1 Torr several spectra are displayed which correspond to different choices of the rotational temperature of the nascent products [Eq. (29)] and of the temperature used in the determination of the downward rates from detailed balancing [Eq. (13)]. We see that there is very little qualitative difference in the predicted spectra. This is satisfying for the following reasons: First, although it is known experimentally that the initial rotational distribution of the nascent CaO products is highly excited,[7] even if it were possible to determine the precise form of this distribution, it would most likely be simplistic to characterize it by a single temperature. However, the relative independence of our model to rotational temperature, at least within the range $4000\ K < T_{rot} < 8000\ K$, implies that our conclusions will be meaningful even if the true CaO* rotational distributions are non-Boltzmann.

It is also clear from the $P=0.3$ and 1.0 Torr traces in Fig. 8 that the predicted spectra are virtually insensitive to the specific choice of the translational temperature parameter which appears in the detailed balancing relationship [Eq. (13)]. The only effect appears to be a slight enhancement in the bandhead and in the short wavelength region, which corresponds to transitions from low J levels of the A state. The effect of a lower value of T_t in Eq. (13) is to proportionally increase the downward rates relative to the upward rates. Thus, we would expect the overall relaxation of the nascent rotational distribution to be more complete at lower values of T_t, which is what we observe in Fig. 8.

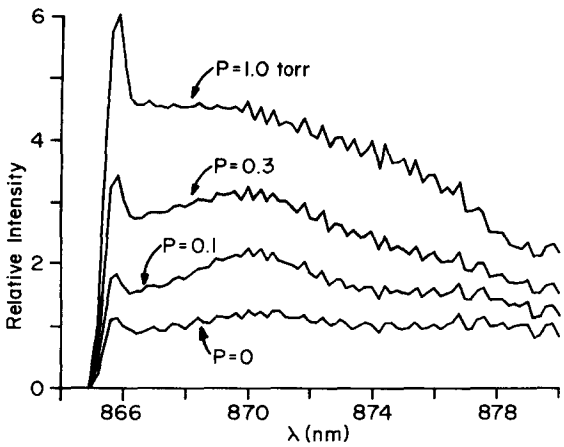

FIG. 9. $A\,^1\Sigma^+(v=0) \rightarrow X\,^1\Sigma^+(v=0)$ band spectra corresponding to an A' to A production ratio [Eq. (29)] of $w=5$. The product rotational temperature [Eq. (29)] was $T_{rot}=8000$ K and the detailed balancing temperature [Eq. (13)] was 1000 K for the spectra at $P=0$ and 0.3 Torr, and 2000 K for the spectra at $P=0.1$ and 1.0 Torr. As in Figs. 7 and 8 the spectra are normalized to the $P=0$ intensity at $\lambda=866$ nm. The zero collision translational loss rate [Eq. (28)] was taken to be 2.55×10^6 s^{-1}, the value appropriate to molecular beam experiments. This figure should be compared with Fig. 8; note, however, that the ordinates are scaled differently.

The small size of this effect seems to indicate that the spectral intensities are most sensitive to collisional transfer of population from the nonradiating A' state, which, within a steady-state approximation, will be insensitive to the specific value of T_t, and less sensitive to rotational relaxation within the A' or A manifolds.

In all the spectra discussed above the ratio of production of the A' and A states was taken to be equal to twice the purely statistical limit, namely $w=2$. Suppose, however, that production of the A' state was favored above and beyond this value due to details of the actual reactive collision dynamics. Figure 9 presents $A(v=0) \rightarrow X(v=0)$ spectra at four collisional pressures for an assumed production ratio of $w=5$. We see the same features as in Fig. 8: perturbational borrowing of intensity from the A' state even at $P=0$, and then at finite pressures direct evidence of collisional $A' \rightarrow A$ transfer in the neighborhood of the isoenergetic point with subsequent radiation in the region of $\lambda=870$ nm. These features are more exaggerated here, when compared with Fig. 8, as are the overall intensities, because of the proportionally greater initial population in the nominally A' state.

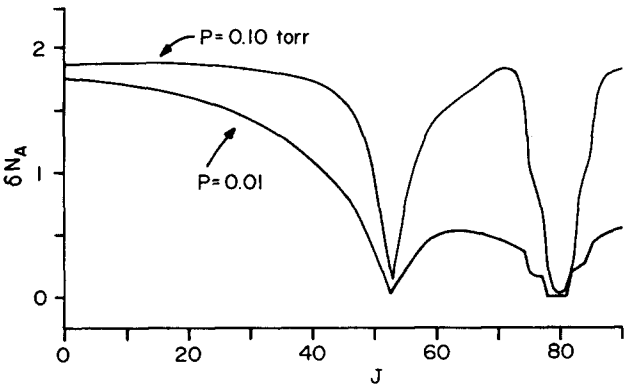

FIG. 10. Relative changes [Eq. (30)] in the population of the mixed Born–Oppenheimer states with an assumed A' to A production ratio of $w=2$ [Eq. (29)]. Values are plotted only for the those levels which are predominately $A\,^1\Sigma^+$ in character; this corresponds to the $|+\rangle$ (lower energy) levels for $J<53$ and the $|-\rangle$ (higher energy) levels for $J>53$. The rotational temperature of the nascent products [Eq. (29)] is 8000 K and the detailed balancing temperature [Eq. (13)] is 4000 K. The zero collision translational loss rate [Eq. (28)] was taken to be 2.55×10^3 s^{-1}, the value appropriate to *flame* conditions. The slight structure around $J=80$ arises from the fact that the $|J,\pm\rangle \rightarrow |J+1,\mp\rangle$ rate constants are very small in this region and have been arbitrarily set to zero whenever their value was less than 1×10^{-11} cm^3/molecule s. This figure should be compared with Fig. 4.

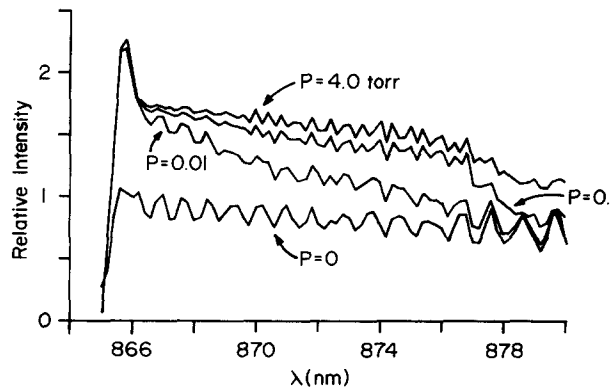

FIG. 11. $A\,^1\Sigma^+(v=0) \rightarrow X\,^1\Sigma^+(v=0)$ band spectra corresponding to an A' to A production ratio [Eq. (29)] of $w=2$. The product rotational temperature [Eq. (29)] is 8000 K and the detailed balancing temperature [Eq. (13)] is 4000 K. All spectra are normalized to the $P=0$ intensity of $\lambda=866$ nm. The zero collision translational loss rate [Eq. (28)] was taken to be 2.55×10^3 s^{-1}, the value appropriate to *flame* conditions. This figure should be compared with Figs. 7 and 8.

IX. POPULATION CHANGES AND SIMULATED CHEMILUMINESCENSE SPECTRA: FLAME CONDITIONS

It is also of interest to consider an experimental situation in which the rate constant for translational loss is much less than the radiative rate of the A state. As discussed in Sec. VI, to simulate this situation we reduced the value of k^0_{loss} in Eq. (13) by a factor of 1000. The resulting relative population changes are displayed in Fig. 10 for a production ratio of $w=2$. In this case, the limiting value of the relative populations [Eq. (31)] is $\delta n_A=2.00$. When we compare Figs. 3 and 8, we observe that substantial increases in population occur at far lower pressures when the translational loss rate is lowered. Most likely this occurs because even at low collisional pressures $A' \rightarrow A$ energy transfer represents the only effective loss channel for the A' state. This is especially true where the orbit-rotation mixing of the states is smallest, at low J, so that the A' levels do not possess any radiative character by virtue of this mixing. This explains the maximum at low J in the curves in Fig. 10.

The corresponding spectra are displayed in Fig. 11.

At low pressures there is clear development of a bandhead. Although the height of the bandhead remains constant at higher pressures, this feature becomes less dominant, as intensity builds up on the long wavelength side. The conventional interpretation would attribute these spectral features to rotational cooling of the nascent A state products with an unexpected rotational heating at higher pressures. Figure 10 enables us to make a more valid interpretation in terms of interelectronic energy transfer. At low pressures the largest change in the steady state populations of the A state levels takes place at low J (Fig. 10). Since the bandhead itself occurs at $J=11$, the net result is a large increase in the intensity of emission at and near the bandhead. At higher pressure population transfer extends to higher values of J (except near the isoenergetic point and in the region where the $A' \rightarrow A$ coupling is negligible). Consequently, the increase in spectral intensity begins to extend to longer wavelengths. We also observe that the overall increase in intensity with increasing pressure is less dramatic than in the case of the high translational loss rate (Fig. 8). This is because the limiting value of the relative population change [Eq. (31)] is significantly smaller when the translational loss rate is much less than the radiative decay rate of the A state.

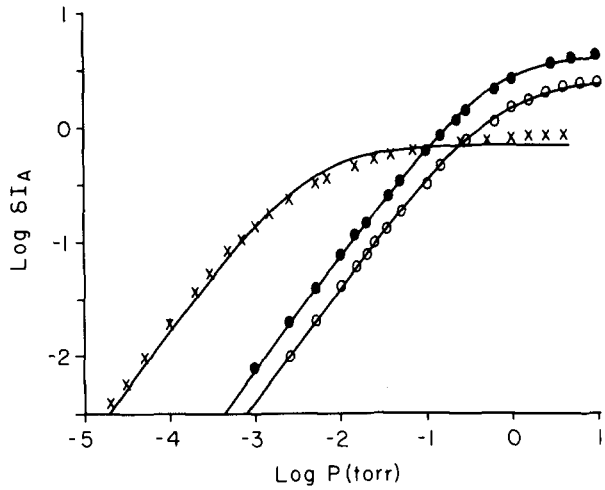

FIG. 12. Relative change in integrated intensity of $A\,^1\Sigma^+(v=0) \rightarrow X\,^1\Sigma^+(v=0)$ emission over the spectra range $865 < \lambda < 880$ nm. The open and filled circles correspond respectively to production ratios [Eq. (29)] of $w=2$ and $w=5$ with a zero collision translational loss rate [Eq. (28)] of 2.55×10^6 s^{-1}. The X's correspond to a production ratio of $w=2$ and a zero collision translational loss rate of 2.55×10^3 s^{-1}. The solid curves represent best minimax fits using the simple two state model presented in the Appendix [Eqs. (A6) and (A12)].

X. PREDICTED INTEGRATED INTENSITIES

In many chemiluminescent reactions the emission is not spectrally resolved, and a measurement is made only of the total integrated intensity for a given vibrational band and/or over a certain spectral bandpass. This type of experiment could be analyzed with a simple two-level kinetic model, similar to the one discussed in the preceding section. In the absence of rotational resolution we shall treat each of the A and A' manifolds as one level with a radiative decay pathway possible only for the A state. The two levels are further assumed initially produced in the ratio $A' : A = w : 1$ and are connected by the collisional rate constant k for $A' \rightarrow A$ transfer and ηk for the reverse $A \rightarrow A'$ process, where η is a parameter. The steady state solution for this simple model is presented in the Appendix, and can be used to predict the relative increase in the rotationally summed A state emission, namely

$$\delta I_A \equiv I_A / I_A^0 - 1 \,, \tag{32}$$

where the superscript naught indicates the integrated intensity in the absence of electronic energy transfer. The specific expression for this relative change in intensity is given by Eqs. (A6) and (A12).

Typically this type of model might be used to fit available experimental data on the pressure dependence of chemiluminescence intensitites and thereby extract values for the rate constant for $A' \rightarrow A$ energy transfer and, possibly for the formation rates of the nascent products. We shall now attempt to determine whether the parameters extracted from this type of fit are physically meaningful. To do so we first integrate $A\,^1\Sigma^+(v=0) \rightarrow X\,^1\Sigma^+(v=0)$ spectra, similar to those presented in Figs. 8 and 9. To remain as faithful as possible to a typical experimental situation, the limits of integration are defined by a particular spectral range, in this case $865\ \text{nm} \leq \lambda \leq 880$ nm, rather than by a range of A state rotational quantum numbers. The resulting relative increases in A state emission [Eq. (32)] are plotted in Fig. 12 for production ratios of $w=2$ and $w=5$ with the fast (molecular beam) zero pressure translational loss rate ($k_{\text{loss}}^0 = 2.55\times10^6$ s^{-1}) and also for $w=2$ with the slow (flame) zero pressure translational loss rate ($k_{\text{loss}}^0 = 2.55\times10^3$ s^{-1}).

The data shown in Fig. 12 were then fitted by minimizing the maximum percentage deviation between the values of δI_A [Eq. (32)] shown in Fig. 12 and the values predicted by the simple two level model presented in the Appendix. We varied not only the two parameters which define the rate of collisional energy transfer, k and η, but also the value of the production ratio w which appears in Eq. (A6). The parameters corresponding to the best "minimax" fit[51] are listed in Table I and the resulting fits to the relative changes in intensity are displayed in Fig. 12.

It is clear that the two level model can provide an accurate fit to the intensity data, certainly to within the resolution of most experiments. For the data corresponding to the fast translational loss rate the fitted values of k, the collisional energy transfer rate constant, are reasonable in view of the magnitude of the actual individual $J \rightarrow J'$ rate constants (Fig. 1) and might be interpreted as an average rate constant, which is consistent with the simplifications which underlie the two level model presented here. However, in the case of the low (flame experiment) value of the zero pressure translational loss rate, the fitted value of the energy transfer rate constant is more than an order of magnitude smaller. This might be rationalized by the observation (Fig. 10) that under these conditions most of the

TABLE I. Fit to pressure dependence of integrated $A\,^1\Sigma^+(v=0) \rightarrow X\,^1\Sigma^+(v=0)$ intensities.

input[a]		best fit[b]		
k^0_{loss}	w	k[c]	η[d]	w[e]
2.55×10^6	2	2.63×10^{-10}	1.23	1.4
	5	2.39×10^{-10}	1.05	2.6
2.55×10^3	2	1.89×10^{-11}	1.0	0.70

[a]Values used in calculation of simulated spectra, units of zero pressure translational loss rate constant are s^{-1}.

[b]Best minimax fit of Eqs. (A6) and (A12) to relative changes in integrated intensity [Eq. (32) and Fig. 12] over the wavelength range $865 \leq \lambda \leq 880$ nm.

[c]Rate constant (cm^3/molecule s) for $A \rightarrow A$ energy transfer.

[d]Ratio of rate constant for $A \rightarrow A'$ energy transfer to the rate constant (previous column) for the reverse process ($A' \rightarrow A$).

[e]Ratio of rate constants for production of A' and A states; this is a free parameter in the fit and is not held equal to the value (column 2) used to simulate the $A \rightarrow X$ spectra.

population change occurs at small J where the $A' \rightarrow A$ transfer rate constants are small, although the actual values are still substantially larger than the fitted value.

It is also significant that the fitted values of the production ratio, w, are much smaller than the values used in the determination of the $A \rightarrow X$ spectra themselves. A reasonable explanation is that not all the rotational levels of the A' state will transfer population to the A state with equal efficiency, which is certainly supported by Figs. 4 and 10. Thus within a simple two level model the ratio of the *effective* A' state population to the total A state population is less than the ratio of the total populations of the underlying rotational manifolds. Also, when the input value of w is raised from $w=2$ to $w=5$, we see in Table I that the fitted value of w does increase, but not by the same factor of 2.5, which we might have expected. The reasons for this are not obvious.

XI. DISCUSSION

We have attempted in this article to develop a kinetic model for collisional energy transfer between dark and radiating excited electronic states of diatomic molecules. The model itself, its implementation, and the resulting predictions have been the subject of the preceding sections of this paper. In the present section we shall discuss both the implications of our work in terms of future experimental studies as well as some possible deficiencies in the theoretical model.

It is clear from the spectra presented in Sec. VIII that inelastic collisions can lead to a substantial degree of population transfer from dark to radiating states if there exist near degeneracies and if the non-Born-Oppenheimer coupling between the two states is reasonably large. This transfer, and even the mixing which is present at zero collisional pressure, can alter the expected spectral features and result in sizeable increases in intensity. Because of this degree of population transfer it can be erroneous to interpret spectral profiles in terms of a rotational temperature of the light emitting state or to interpret changes in these profiles in terms of relaxation processes, rotational or rovibrational, solely among the rotation-vibration levels of the light emitting state.

As an example of how the present study could be used in the understanding of experimental results, we present in Fig. 13 chemiluminescence spectra obtained by Irvin and Dagdigian[8] from the reaction of $Ca(^3P^0)$ with N_2O, at three different N_2O pressures. Both the wavelength range and the spectrometer bandpass are identical to the values used to produce the simulated spectra shown in Figs. 8 and 9. The experimental spectra are complicated somewhat by the large degree of overlap between the various $\Delta v = 0$ sequences in the CaO $A \rightarrow X$ spectra. The heads of the 1–1, 2–2, 3–3, and 4–4 bands all lie less than 1 nm to the red of the 0–0 bandhead. Fortunately, the Franck–Condon factors

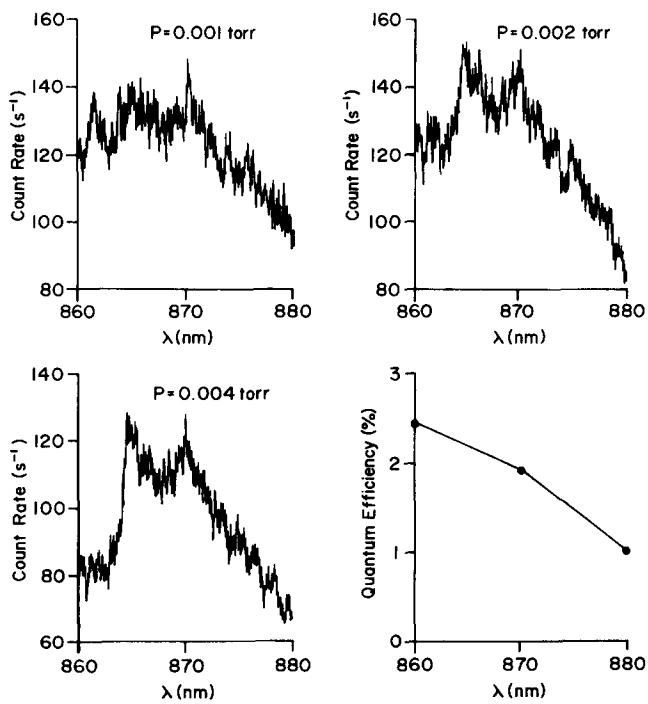

FIG. 13. Experimental chemiluminescence spectrum, taken by Irvin and Dagdigian (Ref. 8), for the reaction of $Ca(^3P^0)$ with N_2O at N_2O pressures of 0.001, 0.002, and 0.004 Torr. The molecular beam experiment is described in Ref. 7. These spectra were taken with a path length (Ref. 7) of $l = 5.8$ cm and a bandpass (FWHM) of 0.5 nm. In all cases the background count rate is ~14 cps. The spectral region displayed contains the CaO $A \rightarrow X$ $\Delta v = 0$ bands. No correction has been made for the overall quantum efficiency (lower right-hand panel) of the spectrometer, photomultiplier, photon counter combination (Ref. 7). These efficiencies were evaluated at the points shown by filled circles, and have been connected only to guide the eye. The spectra shown are higher resolution segments of spectra such as the one displayed in Fig. 5 of Ref. 7, and should be compared, after correction for the efficiency of the detection train, with Figs. 8 and 9 of the present paper.

for these higher bands are substantially smaller than for the 0–0 band,[49] so that the experimental spectra displayed in Fig. 13 consists predominantly of the $A \rightarrow X$ 0–0 band. Bandheads of the $\Delta v = 0$ sequence for $v > 4$ lie to the blue of the 0–0 head so that emission from high vibrational levels of the A state does not contribute to the spectra in Fig. 13.

Qualitatively, the main features of the experimental spectra are similar to those which appear in our simulated spectra, namely the increase, with increasing N_2O pressure, of intensity both at the bandhead and in the region of the perturbation mixing ($\lambda \simeq 870$ nm). It does not appear, however, that a good *quantitative* agreement exists between Fig. 13 and Figs. 8 or 9. In particular the pressure dependent changes in the experimental spectra appear to occur at much lower pressures than would be predicted by our simulation study. Possibly this discrepancy arises from the nature of the experiment. The spectra shown in Fig. 13 were taken with the long path length cell described in Ref. 6 rather than with the pinhole configuration which was used to obtain the low pressure data reported by Irvin and Dagdigian.[6] Thus some A' molecules could have been produced upstream of the observation zone so that the effective translational loss rate for the spectra shown in Fig. 13 should be considerably slower than the value used to produce Figs. 7, 8, and 9. As we have seen, with a lower translational loss rate, transfer from the A' reservoir states occurs at lower values of the collisional pressure.

Another possible explanation for the apparent discrepancy between the pressure dependence of the simulated and experimental spectra is that the A' to A production ratio is even greater than the value of $w = 5$ used to produce Fig. 9. The difference could also reflect the spectral overlap discussed in the paragraph before the last, so that spectral features arising uniquely from population changes in the $v = 0$ level of the A state are obscured by pressure dependent changes in the $v = 1$, 2, 3, and 4 levels.

Obviously, one would like to extract the energy transfer rate constants and the ratio of the nascent product production rates directly from experimental data, or ultimately, by comparing experimental and simulated spectra. The preceding paragraphs suggests that this may not yet be possible, given the degree of experimental resolution presently available and given the possible inaccuracies in a theoretical simulation such as the one presented here. These will be discussed in more detail below. It is important, moreover, to repeat the conclusion of the preceding section, namely that although pressure dependent intensity data can be fit well by simple kinetic models, it is extremely dangerous to attempt to extract meaningful values of the desired rate constants from an experiment lacking at least some degree of rotational state resolution.

It is instructive at this point to compare Fig. 12 of the present article with Fig. 7 of the article by Irvin and Dagdigian,[6] which displays the pressure dependence of the relative yield of $A\,^1\Sigma^+ \rightarrow X\,^1\Sigma^+$ emission following the reaction of $Ca(^3P^0)$ with N_2O. The curves are qualitatively similar except that the rise in experimental intensity occurs at lower pressures than for the curves in Fig. 12 corresponding to the molecular beam translational loss rate. Possibly this difference reflects the fact that the simulated curves represent an integration over a much smaller spectral range. Alternatively, it could be that the present treatment of translational loss is simplistic in the assumption of a uniform velocity for nascent products. Irvin[52] has suggested that with a more reasonable assumption of a distribution of product velocities some of the A' products would have slower translational loss rates, so that significant population transfer, and a consequent rise in integrated intensity, would occur at lower pressures, as in our simulation of the "flame" experiments.

This particular comparison as well as the overall conclusions of Secs. VII–X illustrate the extreme sensitivity of emission intensity to the assumed rate of translational loss. Clearly an accurate description of this (or other) loss mechanisms for both dark and radiating states is critical for the accurate interpretation of experiments. As a corollary, it may be dangerous to compare spectra or photon yields obtained in experiments where differences in design imply that the translational loss of excited state population is sampled differently.

On the basis of the comparison between Fig. 13 and Figs. 8 and 9 we believe that the qualitative conclusions of our study and the experimental implications discussed in the preceding paragraphs are sufficiently general and fundamental that they will be valid regardless of any quantitative shortcomings of our theoretical model. We turn now to a discussion of these. Foremost are errors that might be introduced by inaccuracies in the computed rate constants. These are discussed in I. Obviously, more accurate values could provide a valuable check of the quantitative accuracy of the calculations presented here.

In this paper we have considered only the coupling between the A' and A states. A next level of sophistication would be to consider coupling between the $a\,^3\Pi$ and A states and, ultimately, between all these levels. Only the $\Omega = 0$ fine structure component of the $^3\Pi$ state with e parity is spin-orbit coupled to the $A\,^1\Sigma^+$ state.[21] For CaO it is the $v = 7$ rotational manifold of the $a\,^3\Pi_0$ state which becomes isoenergetic, at $J = 75$, with the $v = 0$ manifold of the A state.[21] Since the statistical degeneracy of the $a\,^3\Pi_0$ component is identical to that of the $A'\,^1\Pi$ state and since the isoenergetic point occurs at roughly the same value of J, we might expect that the effect of collision induced $a\,^3\Pi_0 \rightarrow A$ population transfer will be similar to the $A' \rightarrow A$ transfer examined in the previous section. In the case of CaO we expect the A state population changes due to transfer from the two Π states will be additive, since, as was discussed in I, the direct coupling between the two Π states is expected to be negligibly small.

The present article presents only a steady state solution of the master equation describing population transfer between two excited electronic states. This approach is appropriate for the understanding of molecular

beam or flow type experiments in which the production of these excited states is continuous. We plan soon to carry out the exact solution of the master equation with techniques which have been widely used in the study of vibrational energy transfer.[53–55] This will provide a picture of the time dependence of the population transfer which will aid in understanding experiments in which an intense pulsed laser is used to excite a particular vibration-rotation level of an excited state, and the subsequent energy transfer is probed by laser induced fluorescence involving neighboring levels of the same or a different electronic state.[56] It is our feeling that the greater degree of resolution in this latter type of experiment offers more promise for unraveling the full details of collision induced energy transfer between electronically excited states. The complexity of this process should not be a deterrent to future work, but rather a challenge, one which can best be met by a collaborative attack by experimentalist and theoretician.

ACKNOWLEDGMENT

The author would like to thank his experimentalist colleagues, Paul Dagdigian and John Irvin for their continual encouragement and helpful comments, for permission to use the spectra shown in Fig. 13, and for invaluable discussion of the details of their experimental study (Refs. 6–8). Paul Dagdigian is also thanked for making available an RKR program. Finally, the author is immensely grateful to Gary Pruett for instructive criticism of an earlier version of the manuscript. The research described here was supported in part by the U. S. Army Research Office, Grants DAAG29-78-G-0110 and DAAG29-81-K-0102; and by the General Research Board and Computer Science Center, University of Maryland.

APPENDIX: TWO LEVEL MODEL FOR $A' \rightarrow A$ ENERGY TRANSFER

In this appendix we develop a simplistic model for $A' \rightarrow A$ energy transfer which is used in Secs. VII–X to analyze our more exact calculations. The A and A' rotational manifolds are treated as two levels with formation rates k_f and wk_f, respectively, where in the notation of Eqs. (15) and (16),

$$k_f = \sigma F_b N_T \quad . \tag{A1}$$

We introduce rate constants k for collision induced $A' \rightarrow A$ energy transfer and ηk for the reverse process $(A \rightarrow A')$, where η is a multiplicative constant. The rate equations for the populations of the A and A' states are then

$$\frac{dN_A}{dt} = k_f N_T - N_A(k_{\rm rad} + k_{\rm loss} + N_T \eta k) + N_{A'} N_T k \tag{A2}$$

and

$$\frac{dN_{A'}}{dt} = wk_f N_T - N_{A'}(k_{\rm loss} + N_T k) + N_A N_T \eta k \ , \tag{A3}$$

where w is the ratio of A' to A state production, $k_{\rm loss}$ is the rate constant for translational loss, and $k_{\rm rad}$ is the radiative decay rate for the A state.

In the steady state limit these equations can be easily solved for the A state population. In the zero collision limit, obtained by neglecting the last two terms in Eq. (A2), we find

$$N_A^0 = k_f/(k_{\rm rad} + k_{\rm loss}^0) \ , \tag{A4}$$

where the superscript on the translational loss rate indicates the value appropriate to the zero collision limit [Eq. (28)]. If the collision terms are included the result is

$$N_A = \frac{k_f[k_{\rm loss} + k(w+1)]}{k_{\rm rad} k + k_{\rm loss}[k_{\rm rad} + k_{\rm loss} + k(1+\eta)]} \ . \tag{A5}$$

Thus, the relative change in the A state population is given by

$$\delta n_A = N_A/N_A^0 - 1 = \frac{(k_{\rm loss}^0 - k_{\rm loss})(k_{\rm loss} + k) + k[w(k_{\rm rad} + k_{\rm loss}^0) - \eta k_{\rm loss}]}{k_{\rm rad} k + k_{\rm loss}[k_{\rm rad} + k_{\rm loss} + k(1+\eta)]} \ . \tag{A6}$$

It is worthwhile to examine this expression in several limits. The first is the limit as the translational loss rate $k_{\rm loss}$ becomes negligible compared with the energy transfer rate $N_T k$, which would occur at high target gas pressure. We find

$$\lim_{k_{\rm loss} \rightarrow 0} \delta\eta_A = w + (1+w)\, k_{\rm loss}^0/k_{\rm rad} \ . \tag{A7}$$

The low pressure limit is also of interest. To obtain this we first observe that the translational loss rate [Eq. (28)] can be expanded as

$$k_{\rm loss} = k_{\rm loss}^0(1 - \zeta N_T) + O(N_T^2) \ , \tag{A8}$$

with the coefficient ζ given by

$$\zeta = cRT \ . \tag{A9}$$

Here c is the constant in Eq. (28), R is the ideal gas constant, and T is the translational temperature of the target. Introducing this into Eq. (A6), expanding both numerator and denominator as power series in N_T, and keeping only the leading terms, we obtain the expression

$$\lim_{N_T \rightarrow 0} \delta n_A = N_T \frac{wk_{\rm rad} k + k_{\rm loss}[\zeta + (w - \eta)]}{k_{\rm loss}^0(k_{\rm rad} + k_{\rm loss}^0)} + O(N_T^2) \ . \tag{A10}$$

In this simplistic two level model the total intensity of radiation from the A state is given by

$$I_A = N_A k_{\rm rad} \ , \tag{A11}$$

so the the relative increase in the intensity of emission, defined by Eq. (32), is given by

$$\delta I_A = I_A/I_A^0 - 1 = N_A/N_A^0 - 1 = \delta n_A \ . \tag{A12}$$

[1] C. D. Jonah, R. N. Zare, and Ch. Ottinger, J. Chem. Phys. 56, 263 (1972); A. Schultz and R. N. Zare, *ibid.* 60, 5120 (1974); F. Engelke, R. K. Sander, and R. N. Zare, *ibid.* 65, 1416 (1976).
[2] C. R. Dickson, S. M. George, and R. N. Zare, J. Chem. Phys. 67, 1024 (1977).
[3] D. J. Wren and M. Menzinger, J. Chem. Phys. 63, 4557 (1975); Faraday Discuss. Chem. Soc. 67, 97 (1979).

[4]A. Siegel and A. Schultz, Chem. Phys. **28**, 265 (1978).
[5]P. J. Dagdigian, Chem. Phys. Lett. **55**, 239 (1978); B. E. Wilcomb and P. J. Dagdigian, J. Chem. Phys. **69**, 1779 (1978); L. Pasternack and P. J. Dagdigian, Chem. Phys. **33**, 1 (1978).
[6]J. A. Irvin and P. J. Dagdigian, J. Chem. Phys. **73**, 176 (1980).
[7]J. A. Irvin and P. J. Dagdigian, J. Chem. Phys. **74**, 6178 (1981).
[8]J. A. Irvin and P. J. Dagdigian (unpublished).
[9]C. R. Jones and H. P. Broida, J. Chem. Phys. **60**, 4369 (1974).
[10]C. R. Jones and H. P. Broida, J. Chem. Phys. **59**, 6677 (1973).
[11]R. W. Field, C. R. Jones, and H. P. Broida, J. Chem. Phys. **60**, 4377 (1974).
[12]B. G. Wicke, M. A. Revelli, and D. O. Harris, J. Chem. Phys. **63**, 3120 (1975).
[13]G. A. Capelle, C. R. Jones, J. Zorski, and H. P. Broida, J. Chem. Phys. **61**, 4777 (1974).
[14]A. Torres-Filho and J. G. Pruett, J. Chem. Phys. **70**, 1427 (1979); A. Torres-Filho and J. G. Pruett, *ibid.* **77**, 740 (1982).
[15]D. J. Benard, W. D. Slafer, and J. Hecht, J. Chem. Phys. **66**, 1017 (1977); D. J. Benard, W. D. Slafer, and P. H. Lee, Appl. Opt. **16**, 2108 (1977).
[17]D. J. Eckstrom, S. A. Edelstein, D. L. Huestis, B. E. Perry, and S. W. Benson, J. Chem. Phys. **63**, 3828 (1975); D. J. Eckstrom, J. R. Barker, J. G. Hawley, and J. P. Reilly, Appl. Opt. **16**, 2102 (1977).
[18]C. J. Hsu, W. D. Krugh, and H. B. Palmer, J. Chem. Phys. **60**, 5118 (1974).
[19]E. S. Fleming and H. B. Palmer in *Electronic Transition Lasers*, edited by J. I. Steinfeld (Massachusetts Institute of Technology, 1976), p. 70.
[20]R. W. Field, R. A. Gottscho, J. G. Pruett, and J. J. Reuther, in "Proceedings 14th International Conference on Free Radicals," Sanda, Japan (1979).
[21]R. W. Field, J. Chem. Phys. **60**, 2400 (1974).
[22]K. P. Huber and G. Herzberg, *Constants of Diatomic Molecules* (Van Nostrand Reinhold, New York, 1979).
[23]Throughout this paper we shall use the spectroscopic state labels appropriate to CaO, the molecule which is the subject of our numerical calculations, namely, $a\,^3\Pi$, $A\,'^1\Pi$, $b\,^3\Sigma^+$, $A\,^1\Sigma^+$. For the other alkaline earth oxides the spectroscopic labels occasionally differ. In particular for MgO the four excited states are denoted $a\,^3\Pi$, $A\,^1\Pi$, $b\,^3\Sigma^+$, $B\,^1\Sigma^+$ (Ref. 22); and, for BaO, $a\,^3\Sigma^+$, $A\,^1\Sigma^+$, $b\,^3\Pi$, $A\,'^1\Pi$ [R. A. Gottscho, J. Chem. Phys. **70**, 3554 (1979)].
[24]M. H. Alexander, J. Chem. Phys. **76**, 429 (1982).
[25]J. L. Gole and S. A. Pace, J. Chem. Phys. **73**, 836 (1980).
[26]D. H. Katayama, T. A. Miller, and V. E. Bondybey, J. Chem. Phys. **71**, 1662 (1979).
[27]H. E. Radford and H. P. Broida, J. Chem. Phys. **38**, 644 (1963).
[28]W. M. Gelbart and K. F. Freed, Chem. Phys. Lett. **18**, 470 (1973).
[29]P. J. Dagdigian and M. H. Alexander, J. Chem. Phys. **72**, 6513 (1980).
[30]J. M. Brown, J. T. Hougen, K. P. Huber, J. W. C. Johns, I. Kopp, H. Lefebvre-Brion, A. J. Merer, D. A. Ramsay, J. Rostas, and R. N. Zare, J. Mol. Spectrosc. **55**, 500 (1975).
[31]R. N. Zare, A. L. Schmeltekopf, W. J. Harrop, and D. L. Albritton, J. Mol. Spectrosc. **46**, 37 (1973).
[32]R. A. Gottscho, J. B. Koffend, and R. W. Field, J. Mol. Spectrosc. **82**, 310 (1980).
[33]J. T. Hougen, Natl. Bur. Stand. U. S. Monogr. **115** (1970).
[34]C. G. Gray and J. Van Kranendonk, Can. J. Phys. **44**, 2411 (1966).
[35]H. A. Rabitz and R. G. Gordon, J. Chem. Phys. **53**, 1815, 1831 (1970).
[36]R. D. Sharma and C. A. Brau, J. Chem. Phys. **50**, 924 (1969).
[37]For an excellent review, see G. G. Balint-Kurti, in *International Review of Science, Physical Chemistry* (Butterworths, London, 1975), Ser. 2, Vol. 1.
[38]P. J. Dagdigian, B. E. Wilcomb, and M. H. Alexander, J. Chem. Phys. **71**, 1670 (1979).
[39]See, for example, I. W. M. Smith, *Kinetics and Dynamics of Elementary Gas Reactions* (Butterworths, London, 1980).
[40]See, for example, Ref. 7.
[41]G. Herzberg, *Spectra of Diatomic Molecules* (Van Nostrand, Princeton, 1965), pp. 193–207.
[42]Irvin and Dagdigian (Ref. 7) report a value of 155 ± 60 ns for τ_Σ and estimate that τ_Π is $\sim 10\ \mu$s, comparable to the lifetime of the BaO $A\,'^1\Pi$ state. [S. E. Johnson, Jr., Chem. Phys. **56**, 149 (1972); J. G. Pruett and R. N. Zare, *ibid.* **62**, 2050 (1975)].
[43]H. Rabitz and S. H. Lam, J. Chem. Phys. **63**, 3532 (1975).
[44]A far more sophisticated treatment of the time dependence of translational loss out of an initially formed cloud of molecules at low density is contained in the appendix of an article by J. C. Stephenson and D. S. King [J. Chem. Phys. **69**, 1485 (1978)].
[45]M. H. Alexander and P. J. Dagdigian, Chem. Phys. **33**, 13 (1978).
[46]We are comparing here only the production of two vibrational levels of the $A\,^1\Sigma^+$ and $A\,'^1\Pi$ states which are nearly isoenergetic. The overall production ratio, summed over vibrational levels, will be considerably different if the term values of the two states (T_e) differ significantly. For a complete discussion of statistical models for the reactions of alkaline earth atoms with molecular oxidants, we refer the reader to Ref. 45.
[47]See, for example, L. Pasternack and P. J. Dagdigian, J. Chem. Phys. **67**, 3854 (1977).
[48]Using the CaO dissociation energy of Irvin and Dagdigian (Ref. 6) to compute the exoergicity for the $CaO(^3P) + N_2O$ reaction (Ref. 45), we estimate $J_{max} \simeq 239$ for $A\,^1\Sigma^+ (v = 0)$.
[49]We are indebted to R. W. Field for supplying us with the CaO A–X Franck–Condon factors.
[50]See also p. 281 and pp. 286–292 of Ref. 41 for a general discussion of the effects of rotational perturbations on diatomic spectra.
[51]E. Isaacson and H. B. Keller, *Analysis of Numerical Methods* (Wiley, New York, 1966), pp. 221–226.
[52]J. A. Irvin (private communication, 1981).
[53]H. Rabitz and G. Zarur, J. Chem. Phys. **62**, 1425 (1975).
[54]H. O. Pritchard and N. I. Labib, Can. J. Chem. **54**, 329 (1976).
[55]J. E. Dove, D. G. Jones, and H. Teitelbaum, J. Phys. Chem. **81**, 2564 (1977).
[56]Y. C. Hsu and J. G. Pruett (private communication, 1981).